

Temperature dependence of broadband seismometer sensitivity

Tomofumi Shimoda¹, Wataru Kokuyama¹, and Hideaki Nozato¹

ABSTRACT

Broadband seismometers are widely used in global observation networks deployed for geophysics research. Recently, the calibration of their sensitivity has become an important factor for ensuring observation accuracy. One of the limiting factors of calibration uncertainty is the temperature dependence of the sensitivity because seismometers operate in a wide range of temperatures. However, systems that accurately measure the temperature coefficient in seismometers have not been established. Herein, we develop such a system using a triaxial vibration exciter combined with a thermostatic chamber. Using this system, we calibrated several broadband seismometers (Trillium Compact, Trillium Horizon 360, and CMG-3T) at various temperatures, ranging from $-15\text{ }^{\circ}\text{C}$ to $+45\text{ }^{\circ}\text{C}$. We found that the temperature coefficient was $(0.11 \pm 0.01)\text{ }^{\circ}\text{C}^{-1}$, which can be attributed to the internal magnet of the seismometers. The variation of the phase delay corresponded to a change of less than 2 ms in output time delay. Additionally, we found that the relative frequency response below 1 Hz was stable against temperature variations. These values are useful for evaluating the measurement accuracy of seismometer observation networks.

KEY POINTS

- The sensitivities of three broadband seismometer models exhibited linear variation with temperature, with a coefficient of $(0.11 \pm 0.01)\text{ }^{\circ}\text{C}^{-1}$.
 - Variations of the output delay over $-15\text{ }^{\circ}\text{C}$ to $+45\text{ }^{\circ}\text{C}$ were within 2 ms.
 - Variations of the low-frequency cutoff were within 1 %.
- [Supplemental Material](#)

INTRODUCTION

Evaluating the measurement accuracy of broadband seismometers is important for ensuring the quality of observation data and detecting instrument failure. For example, the Global Seismographic Network (GSN) requires a calibration accuracy of 1 % as part of its design goal (Lay et al. (2002)). In particular, calibrating the sensitivity under the operational state is essential. Such calibration techniques have been developed by both the geophysical and metrolog-

ical research communities. In some calibration techniques, global events, such as normal modes (Davis et al. (2005)) or tides (Davis and Berger (2007)), have been used as reference signals, with globally common or predictable amplitudes. Another approach compares the observed earthquake signal with the expected vibration calculated using a specific model (Kimura et al. (2015); Ekström and Nettles (2018)). The most direct approach is to compare a local vibration signal with the reference seismometer located near the target seismometer (Anthony et al. (2017); Klaus et al. (2024); Kokuyama et al. (2025)). In these studies, the temperature coefficient of the seismometer sensitivity has been considered an important uncertainty factor that affects both the calibration accuracy of the reference seismometer and the stability of the target seismometer during observations. However, accurate methods for evaluating the temperature coefficient in seismometer sensitivity have not been established.

Although a method for measuring the temperature coefficient of accelerometers have been standardized in ISO 16063-34 (International Organization for Standardization (2019)), the corresponding measurement system has been designed for single-axis measurements. Therefore, this method cannot be employed in broadband seismometers, which has three sensing axes, and their installation orientation is fixed. Additionally, the size and weight of typical broadband seismometers ($\sim 30\text{ cm}$ and $\sim 10\text{ kg}$) are larger than those of typical accelerometers; therefore, the capacity of the systems designed to measure

1. National Metrology Institute of Japan, National Institute of Advanced Industrial Science and Technology, Tsukuba, Japan,  <https://orcid.org/0000-0001-6198-1816> (TS)  <https://orcid.org/0000-0002-3843-2883> (WK)  <https://orcid.org/0000-0001-9614-2203> (HN)

*Corresponding author: tomofumi.shimoda@aist.go.jp

Cite this article as T. Shimoda, W. Kokuyama, and H. Nozato (2022). Temperature dependence of broadband seismometer sensitivity, *Bull. Seismol. Soc. Am.* **XX**, 1–8, doi: [00.0000/0000000000](https://doi.org/10.0000/0000000000).

© Seismological Society of America

the temperature coefficient in accelerometers may be insufficient for broadband seismometers. A recent study (Slad et al. (2024)) adopted a temperature testbed approach; the target seismometer was placed inside an insulated box, and the vibration amplitudes of regional earthquakes were compared at different temperatures.

In this study, based on a recently developed environmental testing system (Shimoda et al. (2025)), we propose and develop a method for measuring the temperature coefficient in broadband seismometer sensitivity. Our system combines a triaxial vibration exciter with a thermostatic chamber and applies vibrations to a seismometer at various temperatures. With this configuration, the characteristics of various seismometers can be evaluated systematically within a short period. In the measurement, the output signal of the seismometer is compared with that of reference accelerometers to calculate the absolute midband sensitivity at each temperature. Furthermore, the relative frequency response of the seismometer is also measured using calibration coils. These measurements revealed that the temperature coefficient is commonly about $(0.11 \pm 0.01) \%/^{\circ}\text{C}$, across different types of broadband seismometers, and that the low-frequency cut-off in the millihertz range is stable against temperature variation. Additionally, we quantitatively characterized the temperature dependence of the phase shift or the calibration coil coefficients.

MEASUREMENT METHOD

Figure 1 shows the experimental setup. A thermostatic chamber was fixed on a triaxial vibration exciter, and the seismometer under test (SUT), along with reference accelerometer (REF), was placed inside the chamber. The system applied vibrations along the three orthogonal axis; the temperature inside the chamber varied from -30°C and $+80^{\circ}\text{C}$. In this study, the temperature points were set to -15°C , 0°C , $+15^{\circ}\text{C}$, $+23^{\circ}\text{C}$, $+30^{\circ}\text{C}$, and $+45^{\circ}\text{C}$. The setup was left overnight to allow the SUT temperature to stabilize at each temperature point; then, absolute midband sensitivity calibrations and relative frequency response measurements were conducted at each temperature. The actual SUT temperature was monitored using a thermocouple (with a 1°C uncertainty) attached to the SUT. The power supply, amplifier, and digitizers for the SUT and REF were placed outside the chamber.

Four broadband seismometers were tested as SUTs: two Trillium Compact (TC120, Nanometrics Inc.), a Trillium Horizon 360 (TH360, Nanometrics Inc.), and a CMG-3T (Güralp Systems Ltd.). Note that the relative frequency response measurement was conducted for one of the TC120s because of the limited number of record channels in our digitizer.

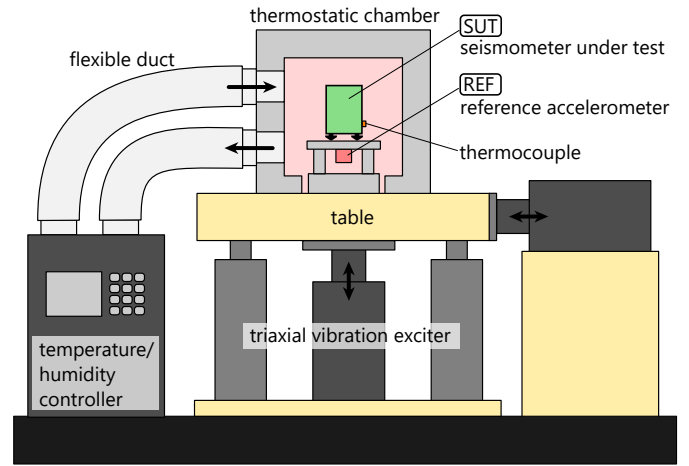


Figure 1. Measurement setup for temperature coefficient of seismometer sensitivity.

Absolute midband sensitivity calibration

To calibrate the absolute midband sensitivity of the SUT, we applied sinusoidal vibrations with a frequency in the 1 Hz–5 Hz frequency range. The output voltage signals of the SUT and REF were recorded using a PXIe-4464 (National Instruments) digitizer, which has an input impedance of 1 M Ω . Then, we calculated the sensitivity of the SUT by comparing the output signal amplitudes as follows:

$$S_{\text{SUT}}(f) = \frac{(2\pi if)\tilde{V}_{\text{SUT}}}{\tilde{V}_{\text{REF}}} S_{\text{REF}}(f), \quad (1)$$

where \tilde{V}_{SUT} and S_{SUT} are the complex amplitudes of the output signal (at frequency f) and the absolute sensitivity (in $\text{V}/(\text{m}\cdot\text{s}^{-1})$ unit) of the SUT, respectively. \tilde{V}_{REF} and S_{REF} are the corresponding parameters of the REF, where S_{REF} is expressed in $\text{V}/(\text{m}\cdot\text{s}^{-2})$ units; thus, a conversion factor $(2\pi if)$ was used to convert acceleration to velocity; this factor is included in the above equation. Finally, the midband sensitivity S_{mid} is defined in this study as the average value of $|S_{\text{SUT}}(f)|$ from 1 Hz to 1.6 Hz, where the frequency response is flat.

In this study, we used three servo accelerometers in x -, y -, and z -axes, respectively, as REFs. Their absolute sensitivities S_{REF} and their temperature dependence were calibrated in advance by applying sinusoidal vibrations and comparing them with a reference laser interferometer included in the measurement system, following a primary calibration method standardized in ISO 16063-11 (International Organization for Standardization (1999)). In the calibration, the REF temperature was varied from -20°C and $+75^{\circ}\text{C}$, and at each temperature the sensitivity was determined by the ratio of the REF output to the reference acceleration measured by the interferometer. Since the interferometer was placed outside the chamber and only its laser beam was introduced into it, the calibration results reflect solely the temperature dependence of the REFs. The measured

temperature coefficient of the REFs ($\sim 0.008 \text{ \%}/^\circ\text{C}$) was corrected during their comparison with the SUT. Estimated relative standard uncertainty of the reference sensitivity ($u(|S_{\text{REF}}|)/|S_{\text{REF}}|$) was 0.15 %. The main uncertainty factors are the accuracy of the voltage measurement, temperature fluctuation, the correction accuracy of the temperature dependence, and reproducibility. Details of the calibration process and its uncertainty have been reported in Shimoda et al. (2025).

To verify the calibration results of the SUT, we conducted validation experiments. Initially, instead of the SUT, we evaluated the same type of servo accelerometer as that used as the REFs. The measured temperature coefficient was $0.004 \text{ \%}/^\circ\text{C}$, which is similar orders of magnitude as the REFs ($0.008 \text{ \%}/^\circ\text{C}$), demonstrating that the measurement procedure is appropriate. Furthermore, in addition to the comparison calibration using the REFs (Eq. (1)), a primary calibration along y -axis was conducted for Trillium Horizon 360 using the laser interferometer, which works as a temperature-independent absolute reference as explained in the previous paragraph. The results of the primary calibration were consistent with those of the comparison calibration within 0.1 %, proving that the REFs did not introduce significant errors. Based on these validations, we concluded that the results shown in the next section are the actual characteristics of the SUTs.

Relative frequency response measurement

The relative frequency response was measured using a calibration coil. The coil and its paired magnet generate an electromagnetic force that simulates the inertial force caused by the ground acceleration. A sinusoidal voltage in the 4 mHz–1 Hz frequency range was applied to the calibration coil, and the equivalent acceleration was calculated using the coefficient of the coil G_{coil} (in $(\text{m}\cdot\text{s}^{-2})/\text{V}$ units), which was obtained from its datasheet. Then, the sensitivity was calculated as follows:

$$S_{\text{SUT,coil}}(f) = \frac{(2\pi if)\tilde{V}_{\text{SUT}}}{G_{\text{coil}}\tilde{V}_{\text{coil}}}, \quad (2)$$

where \tilde{V}_{coil} is the complex amplitude of the calibration input voltage. Again, factor $2\pi if$ was used to convert acceleration to velocity. The normalized value of $S_{\text{SUT,coil}}(f)$ with respect to 1 Hz was calculated as the relative frequency response, which was then fitted to the following transfer function:

$$H(f) = \frac{(2\pi if)^2}{(2\pi if + \alpha + i\beta)(2\pi if + \alpha - i\beta)}. \quad (3)$$

The frequency response of each SUT around the low-frequency pole is given in the datasheet by the above equation; α and β are fitting parameters, which were used to calculate the cutoff frequency $f_c = \sqrt{\alpha^2 + \beta^2}/(2\pi)$.

TABLE 1
Measured temperature coefficients

Sensor		Coefficients ($\text{\%/}^\circ\text{C}$)		
Model	Serial No.	EW	NS	Vert
Trillium Compact	008124	0.113	0.114	0.115
Trillium Compact	008159	0.114	0.112	0.115
Trillium Horizon 360	000790	0.105	0.104	0.106
CMG-3T	T311435	0.100	0.103	0.105

Additionally, by comparing $S_{\text{SUT,coil}}$ with the absolute sensitivity S_{mid} , the absolute value of the coil coefficient G_{coil} can be derived as follows:

$$G_{\text{coil}} = \frac{(2\pi if)\tilde{V}_{\text{SUT}}}{S_{\text{mid}}\tilde{V}_{\text{coil}}}. \quad (4)$$

The comparison was performed using the data in the 1 Hz–1.6 Hz frequency range. We evaluated the temperature coefficient of G_{coil} .

MEASUREMENT RESULTS

Figure 2 shows the measured midband sensitivities. The estimated standard uncertainty of the sensitivity at each temperature was $\sim 0.18 \text{ \%}$, which is dominated by the relative uncertainty of the reference accelerometer sensitivity (0.15 %), the contribution of temperature fluctuation during the measurement (0.1 %), and the voltage measurement accuracy of the digitizer (0.02 %). As shown in Figure 2, the variation of sensitivity with temperature is almost linear for each seismometer. The fitted temperature coefficients are shown in the legend of Figure 2 and summarized in Table 1. The coefficients of the four measured seismometers were similar ($\sim 0.11 \text{ \%}/^\circ\text{C}$); this value is much higher than that of the reference servo accelerometers ($\sim 0.008 \text{ \%}/^\circ\text{C}$). The deviation from the linear fitting shows a small contribution of the higher-order temperature dependency of the sensitivity within $\pm 0.15 \text{ \%}$.

Figure 3 shows the temperature dependence of the phase shift, $\arg(S_{\text{SUT}})$. Since the phase shift depends on frequency, the result at 1.25 Hz is presented as a representative value. As with the midband sensitivity, the phase shift exhibited a linear dependence on temperature with coefficients of approximately $0.001^\circ/\text{C}$, $0.011^\circ/\text{C}$, and $0.005^\circ/\text{C}$ at 1.25 Hz for the Trillium Compact, Trillium Horizon 360s, and CMG-3T, respectively. The frequency dependence of the temperature coefficients is plotted in Figure 4. The coefficients are roughly proportional to frequency and become small in the low-frequency range.

Figure 5 shows the variation of the cutoff frequency fitted from relative frequency response at different temperatures. The Trillium Compact seismometers exhibit a linear dependence with a coefficient of $0.002 \text{ mHz}/^\circ\text{C}$. In contrast, no clear trend in the cutoff frequency variation is

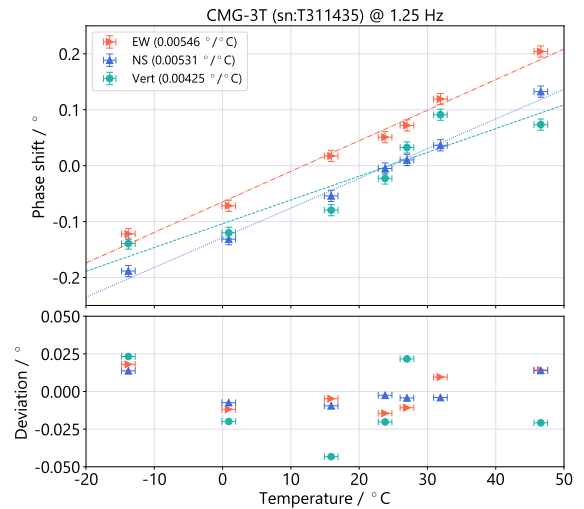
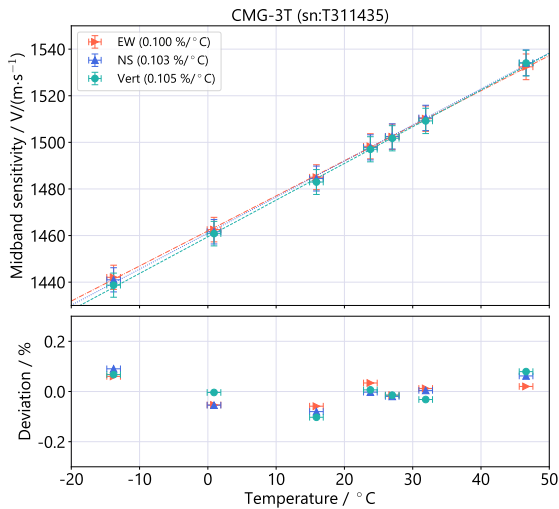
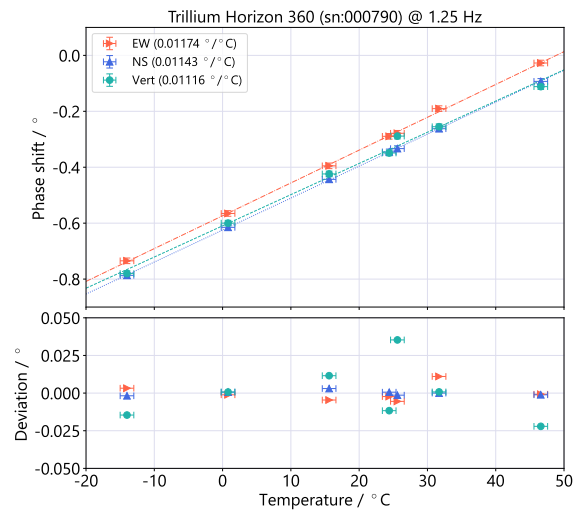
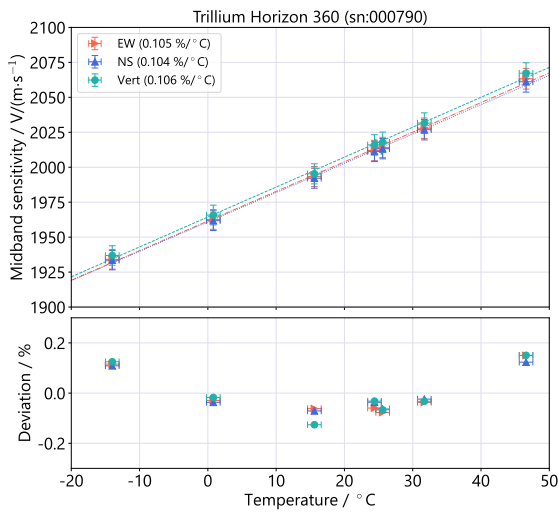
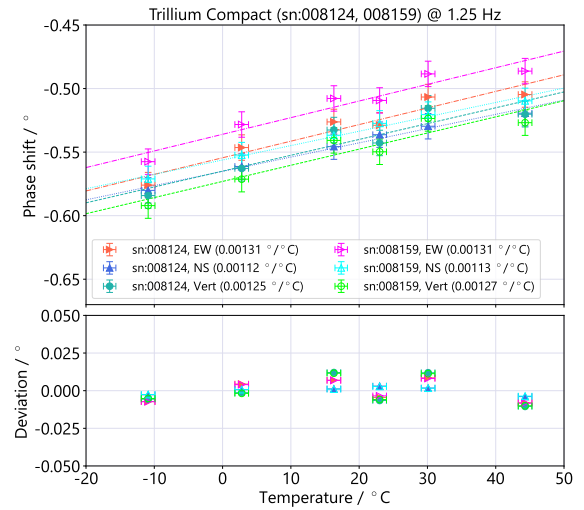
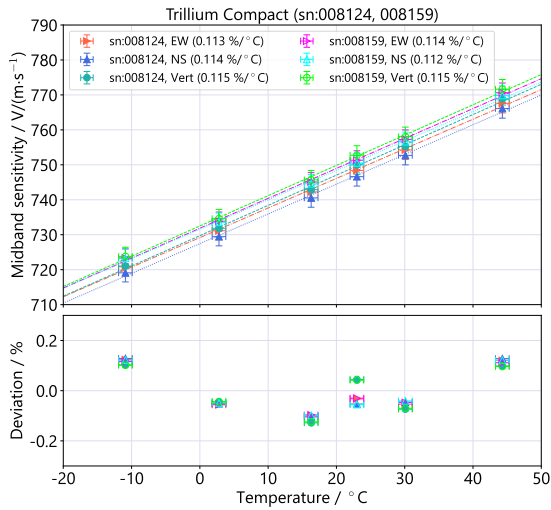


Figure 2. Variation of the midband sensitivity with temperature of the Trillium Compact (top), Trillium Horizon 360 (center), and CMG-3T (bottom) seismometers. The upper half of each graph shows the measured values (points) and their linear fitting (lines). The lower half shows the deviation from the fitting.

Figure 3. Variation of the phase shift with temperature at 1.25 Hz of the Trillium Compact (top), Trillium Horizon 360 (center), and CMG-3T (bottom) seismometers.

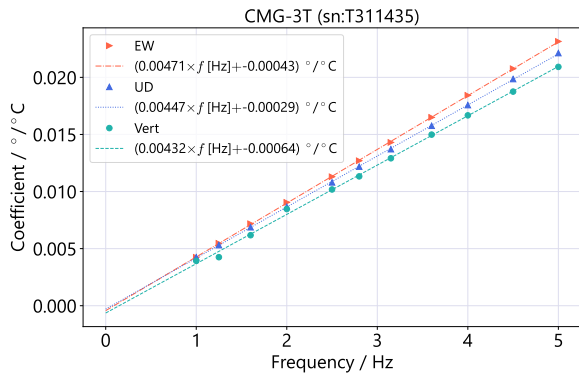
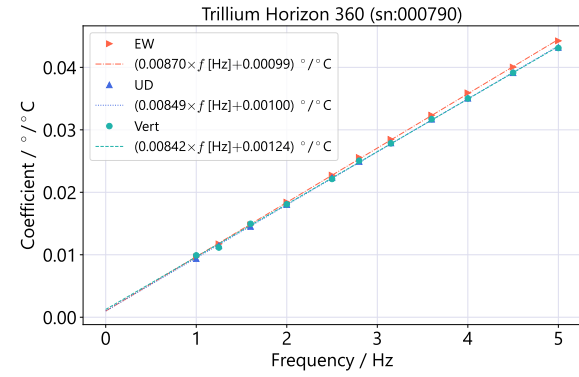
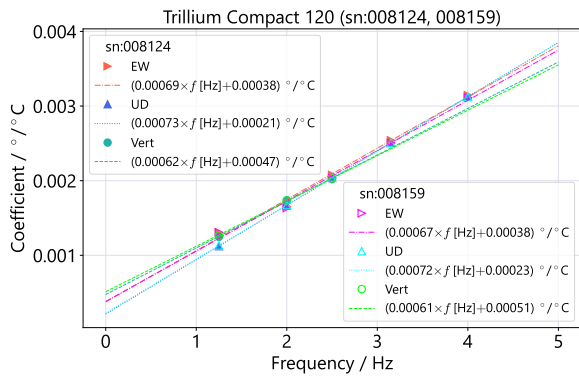


Figure 4. Frequency dependence of the temperature coefficient of phase shift of the Trillium Compact (top), Trillium Horizon 360 (center), and CMG-3T (bottom) seismometers.

observed for the other two seismometers. This might be explained by the large fitting errors caused by the cutoff frequency (≈ 2.7 mHz) being outside the measurement frequency range (> 4 mHz). The deviation over the temperature range (-15 °C to $+45$ °C) was within approximately 1 % of each cutoff frequency.

Figure 6 shows the variation of the calibration coil coefficient with temperature calculated using Eq. (4). We observed that G_{coil} has inverse dependence compared with that of the midband sensitivity. Consequently, the product $S_{\text{mid}} \cdot G_{\text{coil}}$ yields small temperature coefficients of 0.018 %/°C for the Trillium Compact seismometers and 0.002 %/°C for the Trillium Horizon 360 and CMG-3T seismometers. These val-

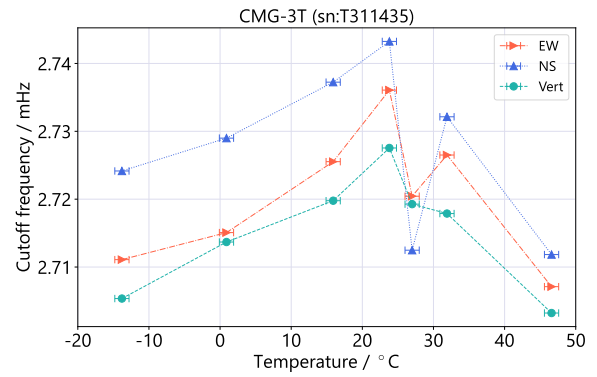
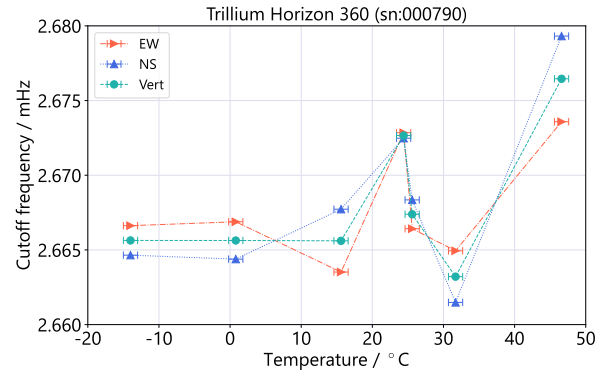
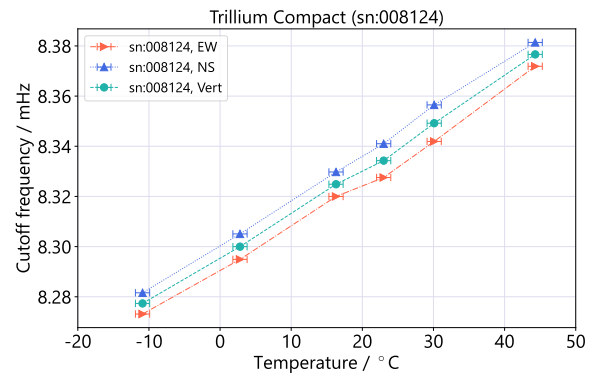


Figure 5. Variation of the fitted low-frequency cutoff frequency with temperature of the Trillium Compact (top), Trillium Horizon 360 (center), and CMG-3T (bottom) seismometers.

ues indicate that variation in G_{coil} is the main source of the temperature coefficient in S_{mid} , as discussed in the next section.

DISCUSSION

The estimated temperature coefficient of the midband sensitivity was (0.11 ± 0.01) %/°C. This value may not be negligible in seismic observations. For example, a temperature difference of 10 °C corresponds to a 1.1 % difference in sensitivity, exceeding the accuracy required by the GSN (Lay et al. (2002)). When a seismometer that has been calibrated in the laboratory is moved to an observation site, its sensitivity should be corrected according to the on-site temperature.

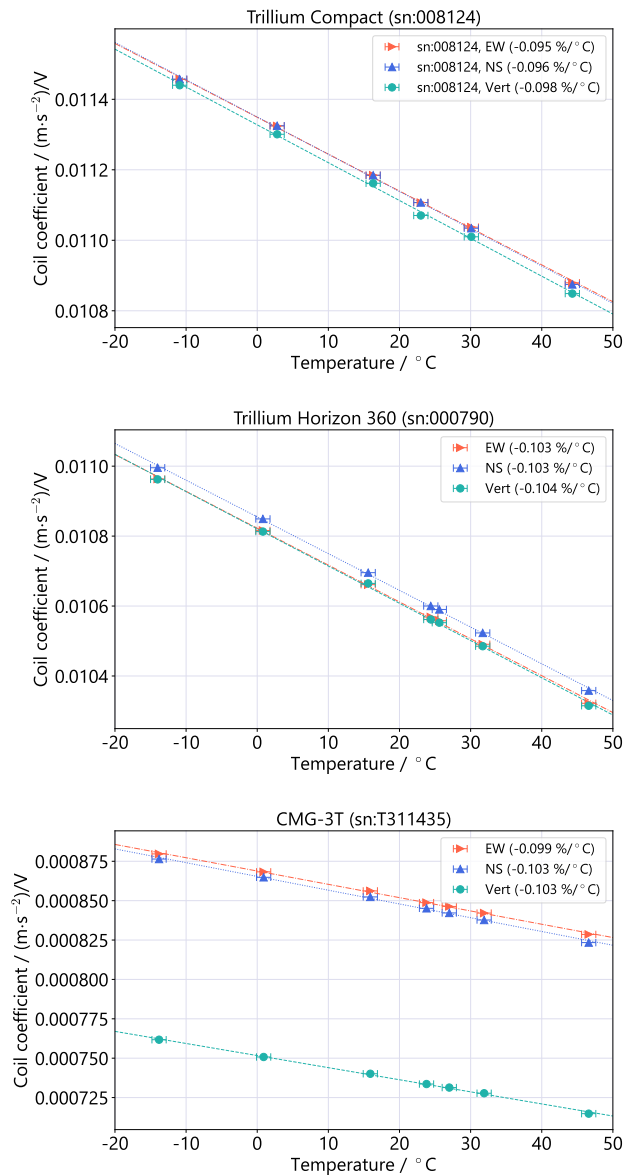


Figure 6. Variation of the calibration coil coefficient G_{coil} with temperature of the Trillium Compact (top), Trillium Horizon 360 (center), and CMG-3T (bottom) seismometers.

Additionally, the temperature coefficient can cause a global systematic difference in the observed vibration amplitude up to a few percent; for example, the temperatures around the equator and the Antarctic differ by a few tens of degrees. Therefore, the temperature at each observation site must be considered to ensure observation accuracy.

Next, we discuss the origin of the temperature dependence. Figure 7 shows a simplified block diagram of a typical broadband seismometer (based on Ackerley (2015); Güralp Systems Ltd. (2023)). The velocity sensitivity is derived as follows:

$$S_{\text{SUT}} = \frac{(2\pi if)V_{\text{SUT}}}{a_g} = \frac{(2\pi if)F_{\text{out}}H}{1 + HFG_{\text{coil}}} \approx \frac{(2\pi if)F_{\text{out}}}{FG_{\text{coil}}}. \quad (5)$$

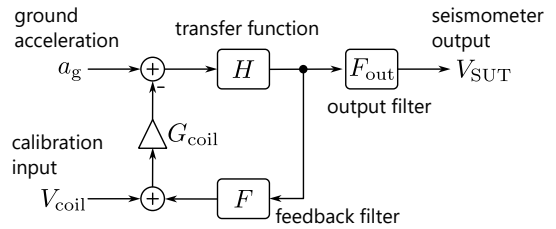


Figure 7. Simplified block diagram of a typical force-balance seismometer. The transfer function H includes a pendulum response, a displacement transducer, and an integrator.

In the above equation, the sufficiently high ($HFG_{\text{coil}} \gg 1$) was used for the approximation. As mentioned in the previous section, the product $S_{\text{SUT}} \cdot G_{\text{coil}} = (2\pi if)F_{\text{out}}/F$ yields a small temperature coefficient. Therefore, the temperature coefficient of S_{SUT} or S_{mid} mainly originates from G_{coil} . The most probable cause of the variation in G_{coil} is the magnet that is paired with the coil; for example, the temperature coefficient of the residual magnetic flux density of an NdFeB magnet ranges from $-0.09 \%/^{\circ}\text{C}$ to $-0.12 \%/^{\circ}\text{C}$ (Trout (2017)). A similar conclusion was reported by Bainbridge et al. (2025). However, further investigation requires detailed information on the component, which is beyond the scope of this study.

The temperature coefficients of the phase shift varied among the seismometers. At 1.25 Hz, the variations over the measured temperature range (-15°C to $+45^{\circ}\text{C}$) were 0.1° , 0.8° , and 0.4° for the Trillium Compact, Trillium Horizon 360, and CMG-3T seismometers, respectively (Figure 3). The corresponding time shifts were 0.2 ms, 1.7 ms, and 0.9 ms. Given the timing accuracy required by the GSN (10 ms), these variations will not seriously matter in broadband seismic observation. For all seismometers, the temperature coefficient was approximately proportional to frequency (Figure 4). This suggests that the variations of the phase shift with temperature may be attributable to high-frequency characteristics of mechanical components or electronics.

The variation in the low-frequency cutoff was small. In the broadband seismometers, the low-frequency cutoff is determined by the feedback circuits composed of resistors and capacitors. Typically, these components have temperature coefficients on the order of 100 ppm/ $^{\circ}\text{C}$, although the value may differ by several factors depending on the specific products. Consequently, they can cause a frequency shift of approximately 0.6% over the temperature range (-15°C to $+45^{\circ}\text{C}$), corresponding to 0.05 mHz for Trillium Compact or 0.02 mHz for Trillium Horizon 360 and CMG-3T seismometers. Considering the uncertainty of the components' temperature coefficients, the results in Figure 5 are consistent with this estimation.

CONCLUSION

Four broadband seismometers were calibrated at different temperatures. The measured temperature coefficient of the midband sensitivity was $(0.11 \pm 0.01) \text{ } \%/^{\circ}\text{C}$, and the relative frequency response was stable against temperature variations. This dependence should be considered when the seismometer operates at temperatures quite different from room temperature ($\sim 23^{\circ}\text{C}$). To ensure observation accuracy within 1 %, the temperature should be monitored within 8°C accuracy. This can be easily achieved using a proper thermometer.

The temperature coefficient of the permanent magnet used as a coil-magnet actuator probably causes a sensitivity variation with temperature; this variation is expected to be consistent across the same-model seismometers. In fact, two Trillium Compact seismometers used in this study exhibited quite a similar temperature coefficients (Figure 2). This can simplify the correction of the temperature-dependent sensitivity because only small number of individuals for each model will need to be characterized. As a next step, we will investigate more seismometers to establish the correction method. Such work can improve the accuracy and reliability of global seismic observation networks.

DATA AND RESOURCES

All measurement data used in this paper were collected by ourselves and are available upon reasonable request.

DECLARATION OF COMPETING INTERESTS

The authors acknowledge that there are no conflicts of interest recorded.

ACKNOWLEDGMENTS

This work was supported by a project commissioned by the New Energy and Industrial Technology Development Organization (NEDO), Japan.

REFERENCES

- Ackerley, N. (2015). *Principles of Broadband Seismometry*, pp. 1941–1970. Berlin, Heidelberg: Springer Berlin Heidelberg.
- Anthony, R. E., A. T. Ringler, and D. C. Wilson (2017, 12). Improvements in absolute seismometer sensitivity calibration using local earth gravity measurements. *Bulletin of the Seismological Society of America* **108**(1), 503–510.
- Bainbridge, G., B. Townsend, and M. Jusko (2025). Field calibration of seismic instruments. Nanometrics Inc.
- Davis, P. and J. Berger (2007, 07). Calibration of the global seismographic network using tides. *Seismological Research Letters* **78**(4), 454–459.
- Davis, P., M. Ishii, and G. Masters (2005, 11). An assessment of the accuracy of gsn sensor response information. *Seismological Research Letters* **76**(6), 678–683.
- Ekström, G. and M. Nettles (2018, 05). Observations of seismometer calibration and orientation at usarray stations, 2006–2015.

Bulletin of the Seismological Society of America **108**(4), 2008–2021.

- Güralp Systems Ltd. (2023). Güralp 3T Operators Guide.
- International Organization for Standardization (1999). ISO 16063-11:1999, methods for the calibration of vibration and shock transducers - part 11: Primary vibration calibration by laser interferometry.
- International Organization for Standardization (2019). ISO 16063-34:2019, methods for the calibration of vibration and shock transducers - part 34: Testing of sensitivity at fixed temperatures.
- Kimura, T., H. Murakami, and T. Matsumoto (2015). Systematic monitoring of instrumentation health in high-density broadband seismic networks. *Earth, Planets and Space* **67**(55).
- Klaus, L., M. Schwardt, C. Pilger, A. Canu, F. Larsonnier, J. H. Winther, N. Tranchant, and A. Havreland (2024). Linking seismic measurements to the international system of units. *Pure and Applied Geophysics* **182**, 5081–5108.
- Kokuyama, W., A. Araya, T. Shimoda, and H. Nozato (2025). On-site calibration of a broadband seismometer. *Measurement: Sensors* **38**, 101752.
- Lay, T., J. Berger, R. Buland, R. Butler, G. Ekström, B. Hutt, and B. Romanowicz (2002). Global seismic network design goals update 2002.
- Shimoda, T., W. Kokuyama, and H. Nozato (2025). Accurate laboratory testing of low-frequency triaxial vibration sensors under various environmental conditions. *arXiv:2512.10771*.
- Slad, G. W., B. J. Merchant, and D. K. Bloomquist (2024). Application of a seismic sensor temperature testbed at sandia national laboratories. Sandia National Laboratories (SNL-NM), Albuquerque, NM (United States).
- Trout, S. (2017). A second look at the reversible temperature coefficients of permanent magnets. Technical report, Spontaneous Materials.

Manuscript Received 00 Month 0000